Received: 25 February 2020 | Revised: 4 June 2020 | Accepted: 18 June 2020

DOI: 10.1002/suco.202000121

fib CEB-FIP WILEY

TECHNICAL PAPER

Probabilistic modeling of reinforcing bar fatigue on the basis of surface topography data

Kai Osterminski

Head of Steel and Corrosion, Chair of Materials Science and Testing, Technical University of Munich, Munich, Germany

Correspondence
Kai Osterminski, Head of Steel and Corrosion, Chair of Materials Science and Testing, Technical University of Munich, Franz-Langinger-Str. 10, 81245 Munich, Germany.
Email: kai.osterminski@tum.de

Funding information
Deutsche Forschungsgemeinschaft, Grant/Award Number: SCHI253/42-1

Abstract

The fatigue of reinforcing bars—as one example of reinforcements in general— is strongly influenced by their surface properties. A lot of research in the 1960s and 1970s has led to the formulation of an analytical model that connects notch stresses to the resulting load cycles in fatigue tests. This article presents the work undertaken in a DFG (German Research Foundation) research project, in which the procedure for assessing the surface properties of rebars with a high-precision laser-linescan system (LLS-system) and subsequently performed fatigue tests were developed. An analytical model was taken as a basis in order to quantify the input parameters and derive the corresponding notch stress factors. The concluding modeling took the scatter into account and allowed for a safety-based recommendation for the derived notch stress factors of reinforcing bars.

KEYWORDS

fatigue, notch stress factor, probabilistic modeling, reinforcing bars, surface topography

1 | INTRODUCTION

The fatigue of reinforcing bars (rebars) depends on three major factors: testing conditions, production-related phenomena, and surface characteristics. Testing conditions are defined by stress levels, amplitude, frequency, and temperature. Whereas amplitude and stress levels are set by standards for testing fatigue behavior (e.g., DIN 488–1[1]), test frequency and temperatures are regulated by DIN EN ISO 15630-1.[2] Concerning production-related phenomena microstructural setup, double skins, grooving, liquation, and especially residual stresses need to be addressed. Most of these phenomena can be minimized by controlling roller ages, cooling temperatures, or melt composition. It is well known, that the surface geometry has the most significant impact on fatigue behavior of rebars. Martin and Schießl[3] showed that fatigue strength was reduced by approximately 60% when ribs were introduced on rebars in the 1960s. More researches, for example, [4–11] examined the effect of ribs on the fatigue strength of rebars and came to the conclusion that the size of the ribs and the design of transition from rib valley to the rib incline—the notch/fillet–are decisive. These findings state that fatigue failure—when not originated by surface phenomena—is caused by deviation of tensile stress trajectories into the rib and the increase of notch stress at the foot joint of the ribs. MacGregor et al.[5] and Jhamb[6] introduced the stress concentration factor k_T (−) for rebars, Equation 1:

Discussion on this paper must be submitted within two months of the print publication. The discussion will then be published in print, along with the authors' closure, if any, approximately nine months after the print publication.

$$k_T = \frac{\sigma_{max}}{\sigma_{nom}}, \quad (1)$$

where σ_{max} (N/mm^2) is the maximum or peak stress at the notch and σ_{nom} (N/mm^2) is the nominal stress in the rebar cross section. Further, the crucial geometrical parameters influencing the stress concentration factor were identified by computer simulations in Jhamb[6] which were incorporated in an analytical relationship by Schießl,[12] Equation 2:

$$k_T = 1 + (0{,}096 - 0{,}12 \cdot \ln(r)) \cdot \sqrt{(b_K + 2 \cdot a \cdot \cot(\alpha)) \cdot (3 + \tan(\alpha))} \quad (2)$$

where r (mm) is the fillet of the notch, b_K (mm) is the width of the rib top, a (mm) is the height of the rib, and α (°) is the angle of the rib slope. It should be noted, that Equation 2 is not consistent considering the units. By definition, all of those geometrical parameters lie in direction of tensile stress trajectories (rebar length axis) when loaded. Figure 1 illustrates the localization of the geometrical parameters in a side view of a rib.

The measurement of geometric parameters and further fatigue experiments in Reference 12 allowed deriving a connection between the born load cycles and the stress concentration factor, Equation 3.

$$\log(N) = f_0(\text{Material, Load}) - f_1 \cdot k_T, \quad (3)$$

where N (−) is the number of load cycles born by the specimen, f_0 (−) is the regression parameter for the influence of loading regime and material properties as well as f_1 (−) which is a regression parameter for the influence of the stress concentration factor originating from the geometrical situation at the failure localization. Schießl[12] stated that values for f_1 would lie between 0.8 and 1.5.

The current paper presents and discusses the experimental investigations involving the surface measurements by laser triangulation using the developed laser-based linescan system (LLS-system)[13] and the corresponding fatigue tests. The understanding of the impact of surface properties on the fatigue behavior of rebars under laboratory testing conditions was the motivation of the presented test series. Thus, the aim of the paper is the quantification of the input parameters for the surface-based analytical equations presented above. All the work was carried out in the course of a DFG (German Research Foundation) research project.

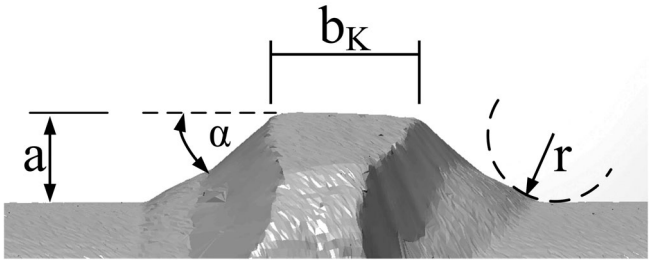

FIGURE 1 Side view of a rebar rib with definition of geometrical parameters (compare Equation 2)

2 | EXPERIMENTAL

2.1 | General

A suitable strategy for a quantification of all input parameters in the notch stress factor equation (Equation 2) and the regression parameters to relate to the fatigue behavior of B500 B rebars (Equation 3) were developed. In order to obtain a widespread and representative data basis, a total of 196 specimens with diameters 16 and 28 mm were investigated, compare Figure 2. A set of specimens was tested for each diameter in order to characterize their mechanical strength. A universal tensile testing machine (ZWICK Roell Z600, Figure 3 left) was used for these tests. The results are given for material characterization in Table 1. The chemical composition of the rebars was tested by glow-discharge optical emission spectroscopy. The given compositions allow for the derivation of the carbon equivalent value of CEV = 0.435 for diameter 16 mm and CEV = 0.444 for diameter 28 mm. The chemical composition is given in Table 2. Both, the mechanical results and the chemical composition are in good agreement with the standards[1] requirements.

The specimens were scanned by the LLS-system resulting in a set of line scan ASCII files containing the longitudinal coordinate X and the corresponding measurement result Y (distance from rebar center to surface). The LLS-system moves a Class 2 laser alongside the rebar length axis. After finishing one line-scan, the LLS-system rotates the rebar repeating the scan process and creating the next line-scan file. The number of the line-scan files represents the rotational position of the scan (rotational angle γ). The LLS-system is capable of measuring with an accuracy of ±1.6 µm in Y-direction, whereas all other

FIGURE 2 Rebar specimens for fatigue testing

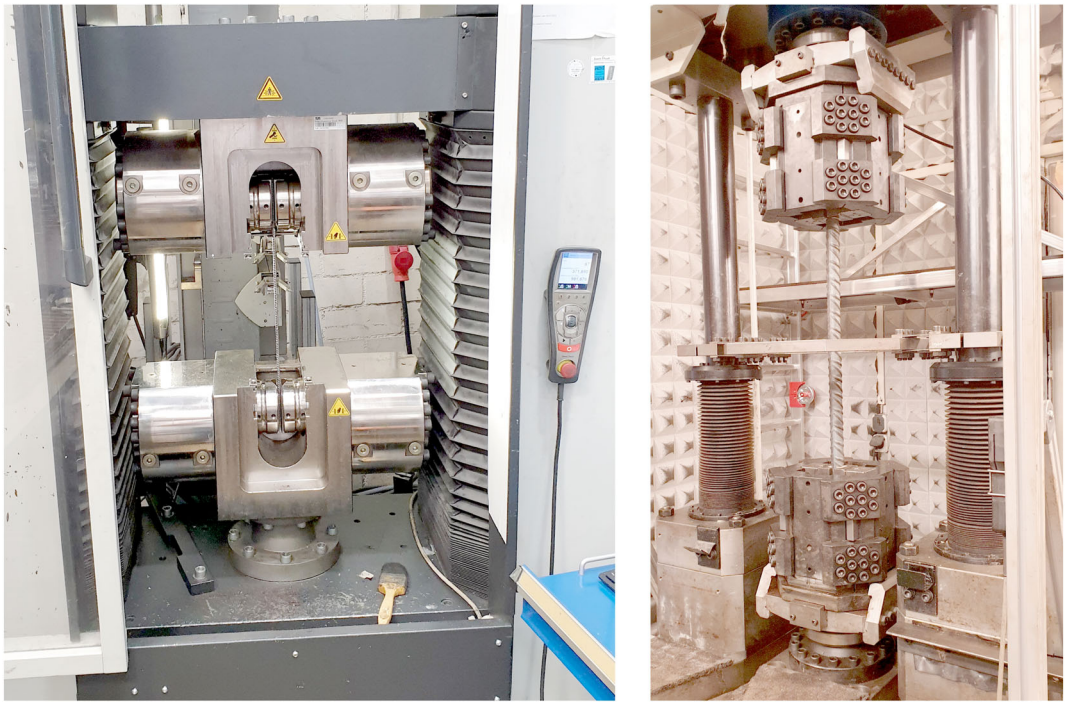

FIGURE 3 Machines applied in testing; left: Uniaxial tensile testing machine depicted with a smaller specimen than investigated in the research; right: Resonance fatigue testing machine

TABLE 1 Results of tensile testing

Diameter (mm)	Parameter/unit (–)	Quantity (–)	Mean value	*SD*
16	R_e (N/mm^2)	17	547	19
	R_m (N/mm^2)	18	654	18
	A_{gt} (%)	18	12.7	1.3
28	R_e (N/mm^2)	18	560	14
	R_m (N/mm^2)	18	672	15
	A_{gt} (%)	18	13.2	1.2

dimensions (position X and rotational angle γ) are considered exact due to the high quality of the selected positioning stepper motors.[13] For a further processing, the raw data needed to be mathematically processed (compare next section). In order to minimize the calculation effort, a suitable measurement strategy was developed, Figure 4.

Primarily, the rebar specimens were prepared by marking on the surface for analyzing the scan files on the digital twin. One hole was center-punched on top of a rib to mark the point of origin (starting point) for each rebar scan. The bottom of the center punch was calibrated before a full surface scan of the rebar was executed. This procedure allowed for a localization of surface phenomena in the scan files. As the punched hole is located on top of the rib with a depth of approximately 100 µm, a notch stress problem and further an impact on the fatigue behavior of the rebar when tested afterward could be excluded.

After scanning, the rebars were tested in an uniaxial tensile–fatigue test until failure. The machine applied in the fatigue tests was a resonance testing machine RUMUL Vibroforte (Figure 3 right). The boundaries of DIN EN ISO 15630-1[2] and DIN 488–1[1] with an upper stress level $\sigma_o = 300$ N/mm^2 (60% of yield strength R_e) and frequency $f \leq 200$ Hz were complied. The test frequencies lay between 74 and 89 Hz in dependence of resonance of the specimen and clamping effect. The fatigue results were sorted into "valid" and "invalid" results by the means of usability for the task of quantifying the input values of presented formulae (Equations 2 and 3). Considering valid results, the failures needed to be subcategorized into causes, such as geometry and surface defects-triggered failures. The invalid results were

TABLE 2 Results of chemical analysis by glow-discharge optical emission spectroscopy

Element (mm)	Diameter 16 mm (wt%)	Diameter 28 mm (wt%)
C	0.187	0.192
Si	0.288	0.285
Mn	0.95	0.97
P	0.017	0.018
S	0.039	0.037
Cr	0.075	0.081
Mo	0.037	0.034
Ni	0.162	0.154
Al	0.002	0.002
Co	0.012	0.011
Cu	0.372	0.366
Nb	<0.002	<0.002
Ti	<0.002	<0.002
V	<0.002	0.002
W	<0.005	<0.005
N	0.0084	0.0088

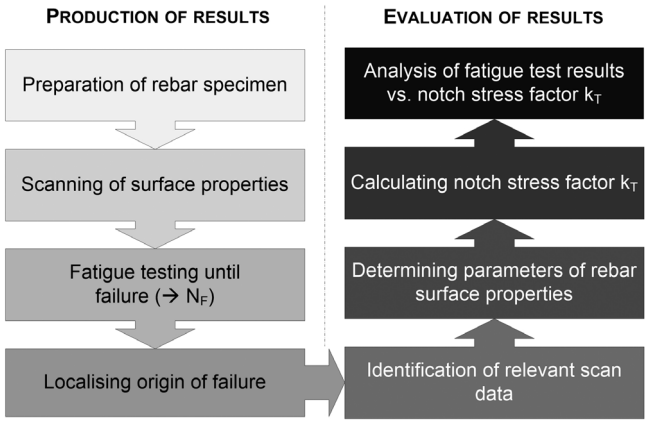

FIGURE 4 Experimental strategy for quantifying the notch stress dependency of the fatigue behavior of rebars

runouts or specimens that failed in proximity to the testing machines bearing.

The specimens with identified geometry-triggered failures were used to determine the rib geometry parameters. Therefore, the origin of failure was located in relation to the starting point (center-punch). The localization was transferred to the digital twin that was produced by the LLS-system. Once located, the surface parameters (a, α, b_K, r) for the rib geometry as it was before testing could be determined as shown in the next

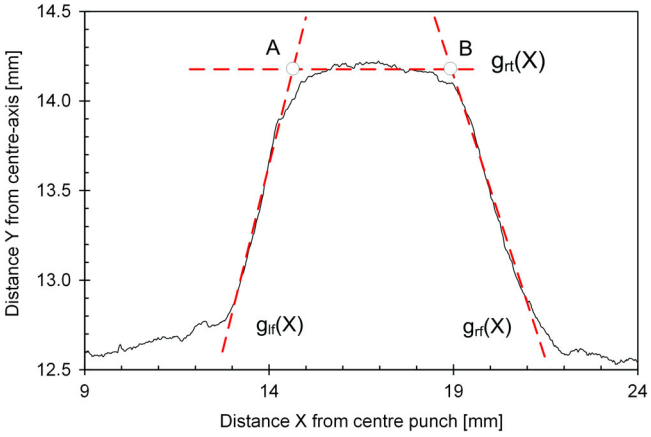

FIGURE 5 Scan result of a rib including fitted linear functions for rib flanks ($g_{lf}(X)$: left flank; $g_{rf}(X)$: right flank) and rib top $g_{rt}(X)$ as well as their intersections A, B

section. The stress concentration factor k_T was calculated on the basis of these surface parameters. Finally, all existing values were categorized in results of the same stress range. Thus, k_T and N were evaluated for the same stress ranges.

2.2 | Mathematical processing of LLS-system data

The surface parameters were determined based on line-scan files, such as presented in Figure 1. Calculation of rib height a is defined in DIN EN ISO 15630-1.[2] Therein, a equals the difference between the maximum value Y_{max} on the rib top scanned in a line-scan and the minimum value Y_{min} of the associating rib trough. This can easily be adapted on the line-scan results. For the calculation of width of the rib top b_K, the rib sections (flanks and top) must be identified first. This is done by fitting linear equations to the scanned rib sections (top, left, and right flank) as shown in Figure 5.

The linear functions for the left rib flank $g_{lf}(X)$ and the rib top $g_{rt}(X)$ intersect in Point A. The intersection of $g_{rt}(X)$ and the function of the right flank $g_{rf}(X)$ are located at Point B. Once the coordinates of the intersections A and B are determined, their horizontal distance can be considered as width of rib top b_K. The angles of the rib slopes α_{lf} and α_{rf} (for definition see Figure 1) can be calculated by solving the arc tangent of the incline/decline of the corresponding linear functions $g_{lf}(X)$ or $g_{rf}(X)$, respectively.

Determination of the radius r needs a fitting of the circle function (Equation 4) to the measuring results in the foot point of the rib. For the circle function, the coordinates of the centre point (X_M, Y_M) have to be determined

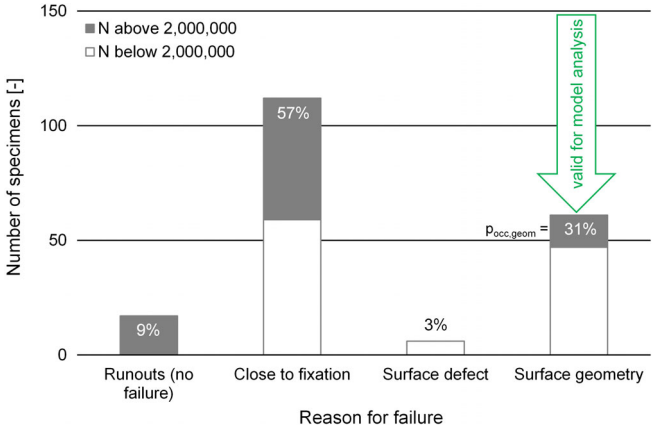

FIGURE 6 General overview of fatigue results

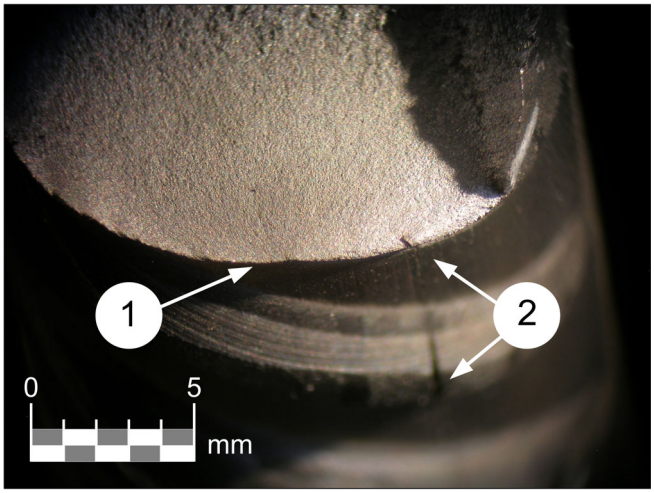

FIGURE 7 Close up of crack face (1: origin of failure; 2: surface defect without impact on failure)

as regression parameters. The coordinates X and Y are taken from the scan results of the notch and implemented in an iteration algorithm that solves for X_M and Y_M as well as the desired radius r.

$$r^2 = (X - X_M)^2 + (Y - Y_M)^2 \tag{4}$$

3 | RESULTS

Figure 6 shows an overview of all fatigue results in the research project. In addition to the absolute numbers of test results the relative figures are given.

The dominant result in the fatigue tests is the rupture/failure of the specimens in proximity to the fixation of the testing machine. It is well known that the triaxial tension situation at the fixation leads to local overstressing of rebars and consequently to failure. The production of rebars might lead to defects on the rebar surface (compare No. 2 in Figure 7) which increase notch stresses. If it is sufficiently high, the notch stresses can initiate micro cracking and a propagating fatigue failure. Figure 6 shows that surface defects played a rather minor role for the investigated rebars. It must be stated, that the percentage can be significantly higher depending on the production parameters of the rebars, for example, the surface of decoiled and straightened reinforcing steels has more defects and might alter the proportions of these findings. Despite extensive testing of up to $20 \cdot 10^6$ load cycles, 9% of all specimens did not fail.

The remaining results failed due to the impact of the surface geometry (compare No. 1 in Figure 7: foot point of a rib). In comparison to the other results it was the second most important failure source in laboratory testing. Considering reinforced concrete, the problem of fixation

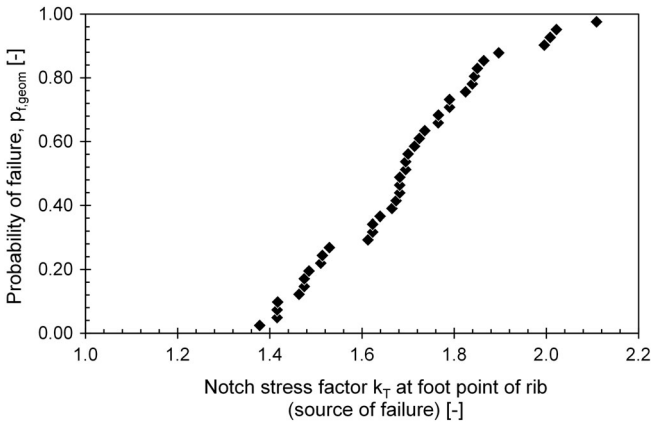

FIGURE 8 Probability of failure in relation to the corresponding notch stress factors located at the source of rebar fatigue failure

is insignificant in situ. With regard to the quantification of modeling parameters in k_T, f_0, and f_1 in Equations 2 and 3 these results can be considered as valid. Therefore, geometrical parameters, stress range $2 \cdot \sigma_a$ and the load cycles N were taken into account. Primarily the stress concentration factors k_T were calculated. The results are given as a cumulated frequency plot in Figure 8. The cumulated frequency can also be understood as probability of failure caused by geometry $p_{f,geom}$.

The calculated mean value for the notch stress factor k_T in the results was 1.69 accompanied by a minimum value of 1.38 and a maximum value of 2.11. Further, the regression factor f_0 was quantified depending on the testing parameter stress range Figure 9 (left). Finally, the regression factor f_1, also called weighing factor of k_T, is quantified, compare Figure 9 (right).

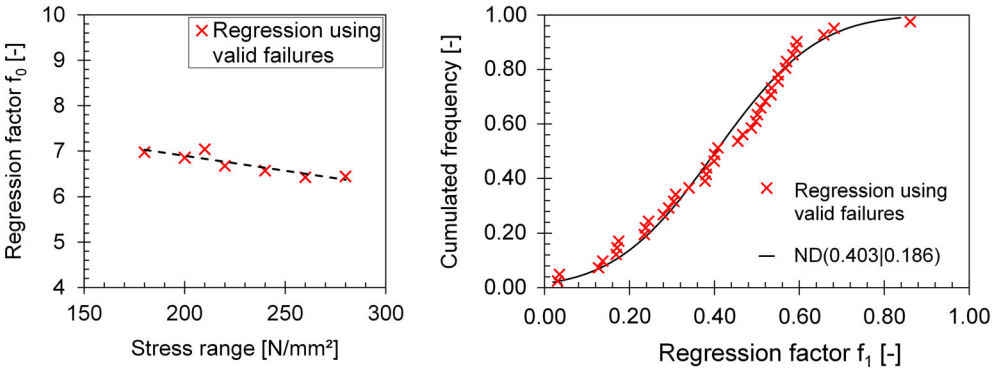

FIGURE 9 Quantification of the regression factors f_0 and f_1 in Equation 3 (left: Regression factor for impact of load regime; right: Weighing factor for k_T as normal distribution [ND])

TABLE 3 Results of regression factor quantification, given parameters refer to normal distribution

Regression factor (–)	Parameter (–)	Values (–)
$f_0 = m_{f0} \cdot (2 \cdot \sigma_a) + b_{f0}$	Slope m_{f0} mean value	−0.0066
	SD	0.0016
	Intercept b_{f0} mean value	8.2166
	SD	0.3838
f_1	Mean value	0.4038
	SD	0.1869

It was stated by Schießl[12] that f_0 is influenced by material and load regime. As the investigated material is of the same quality of rebar (B500 B), the observed variation must be caused by the variation of the stress range. The results of quantification show good accordance between the linear relationship of f_0 and stress range. With an increase in stress range a slight decrease in f_0 can be found. The regression factor f_1 can best be described by a normal distribution (ND). Different distribution types have been investigated (e.g., logarithmic-ND, Weibull, Gumbel, etc.). The ND was calculated to fit best for all input factors of the modeling function in Equation 3. The quantification of the linear function can be found in Table 3. The results for f_1 lie out of the range that was estimated in Reference 12, which were only based on a few test results of no longer state-of-the-art rebars.

3.1 | Modeling

The full probabilistic modeling was processed by implementing f_0 and f_1 in Equation 3. As result, the reachable load cycles N_{max} were calculated. By implementing f_0 and f_1 as scattering parameters, N_{max} scattered as well. Figure 10 shows the results of probabilistic modeling. Herein, the reachable load cycles N_{max}

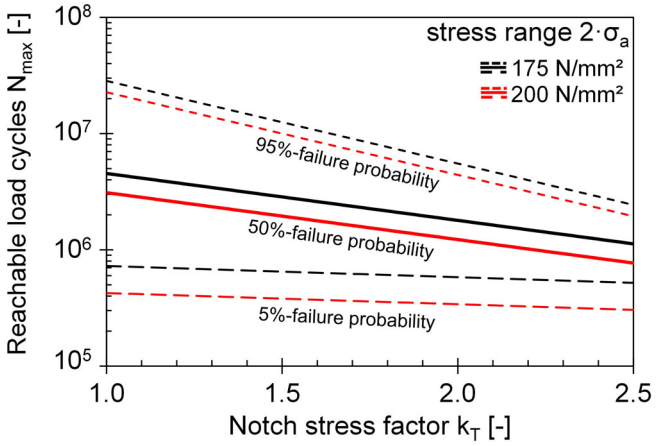

FIGURE 10 Results of probabilistic modeling by implementing the regression factors f_0 and f_1 as well as the notch stress factors k_T (all parameters depicted in Figure 7 and given in Table 1)

are plotted over the notch stress factor k_T. The black lines represent the results for a stress range of 175 N/mm^2 and the red ones for a stress range of 200 N/mm^2. The different shapes of lines depict various failure probabilities in the uniaxial fatigue test.

It can be seen that an increase in k_T results in a decrease in reachable load cycles. The 5% failure probability lines are insignificantly influenced by the notch stress factor. For a notch stress free condition ($k_T = 1.0$) load cycles N_{max} of approximately 725,000 (for $2 \cdot \sigma_a = 175$ N/mm^2) or 425,000 (for $2 \cdot \sigma_a = 200$ N/mm^2) were reached, respectively. These reachable load cycles seem to be quite low. It must be taken into account that a direct comparison to the requirements of standards, for example, DIN 488–1[1] knee point at $N = 1{,}000{,}000$ with $2 \cdot \sigma_a = 175$ N/mm^2 ($p_f = 5\%$ with $W = 0.75$) is not possible, due to the fact that the presented results only deal with a fraction of all specimens investigated— leaving out those that broke in the fixation and those without failure (compare Figure 6: $p_{occ,geom} = 31\%$). For a better understanding, the parameter study was evaluated for the statistical distribution of notch

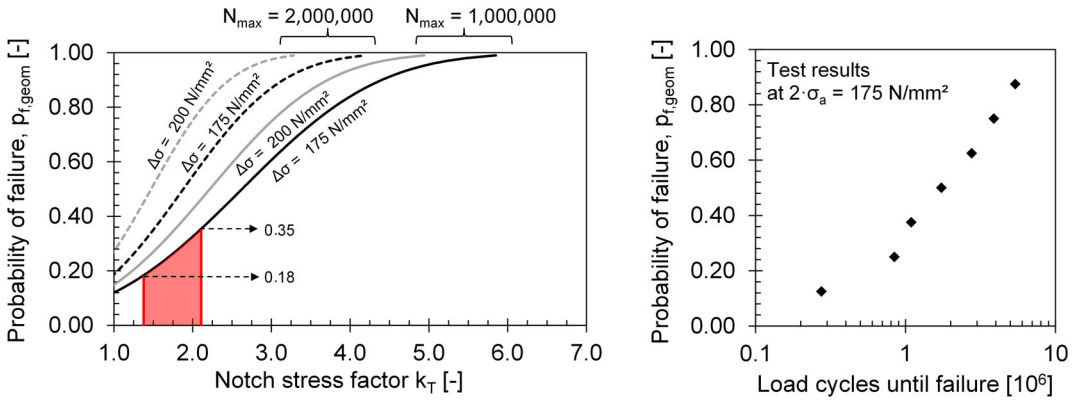

FIGURE 11 Probability of failure depending on notch stress factor for different stress ranges and reachable load cycles (left); Fatigue test results probability of failure over load cycles for a stress range of 175 N/mm^2 (right)

stress factor at N_{max} = 1,000,000 (knee point of the design Wöhler curve) and 2,000,000 (run-out criteria) for the stress ranges of $2 \cdot \sigma_a = 175$ and 200 N/mm^2. Figure 11 (left) shows the results of this evaluation. In addition, the range of k_T which was observed in this research is highlighted. For comparison, the load cycles of all specimens which failed due to the surface geometry at a stress range in experiments of $2 \cdot \sigma_a = 175$ N/mm^2 are shown in Figure 11 (right).

Following Figure 11 (left) the notch stress factors for all rebars investigated in this research can be connected to a modeled probability of failure between 18 and 35%. Naturally, the range of probability of failure (18–35%) can be associated to a range of N between 700,000 and 1,100,000 in the test results which were used to quantify the model parameters, in Figure 11 (right). For taking into account that the probability of occurrence for the failure caused by surface geometry is known, Equation 5 can be applied for calculating the total probability of failure.

$$p_{f,\text{tot}} = p_{f,\text{geom}} \cap p_{\text{occ,geom}}, \tag{5}$$

where $p_{f,\text{tot}}$ is the total probability of failure, $p_{f,\text{geom}}$ is the probability of failure caused by geometry, and $p_{\text{occ,geom}}$ is the probability of occurrence of failure caused by geometry. Consequently, the total probability of failure of the investigated specimens lies between 6 and 11%.

Concluding the test results and calculations it can be stated that the notch stress factor is a decisive parameter for judging the fatigue behavior of rebars. It can be seen from Figure 11 (left) that based on the 196 specimens investigated, a k_T of less than 1.25 would result in a low probability of failure ($p_{f,\text{geom}} < 16\%$ and $p_{f,\text{tot}} < 5\%$). The relationship between k_T and the geometrical parameters is given in Equation 2. Therein, the definition of the geometrical surface parameters a, b_k, and α can be taken from standards DIN 488–2.[14] The remaining parameter which is not defined by aforementioned standard is the decisive notch radius r. Implementing the desired value for $k_T = 1.25$ and the recommended values for the surface geometrical parameters yields the minimum value for the notch radius r_{min}. For a diameter 16 mm rebar a value of $r_{\text{min}} = 1.31$ mm and for a diameter 28 mm rebar; $r_{\text{min}} = 2.20$ mm should not be underrun.

4 | CONCLUSIONS AND OUTLOOK

The current paper reports about the research carried out in a DFG research project. One of the topics of abovementioned project was quantifying the impact of surface geometry on the fatigue behavior of rebars. The developed measurement strategy is presented as well as numerous measurement results. A quantification of surface geometry parameters and input parameters of an analytical model from the 1970s resulted into a detailed analysis for a high number of specimens. These results allow for the following conclusions:

1.Surface scan results of reinforcing steel bars allowed for the calculation of surface parameters needed for implementation in an existing analytical formula for the calculation of notch stress factors k_T.

2.The fatigue behavior of the scanned specimens was investigated in uniaxial tensile load fatigue tests. The surface geometry by the means of the notch stress factor k_T could be correlated with the fatigue test results (load cycles N) applying the analytical formula.

3.Probability of failure in fatigue tests was correlated to notch stress factors. A low probability of failure of 5% was associated with a maximum notch stress factor of 1.25. This maximum notch stress factor can be achieved by staying within the geometrical recommendations of

standards and increasing the notch radius. For a diameter 16 mm the notch radius needs to exceed 1.31 mm and for a diameter 28 mm 2.20 mm.

For future application of the LLS-system it is important to implement the scan data into 3D-Finite Element Method (FEM) analysis as a digital twin to achieve a deeper understanding in the development of notch stresses. In particular, the 3D distribution of tensions in the area of the rebar surface must be investigated. Therefore, beside the surface properties different information about metallurgical and chemical composition as well as residual stress distributions need to be taken into account. Aim of such research could be for example, a reduction in the observed high scatter of fatigue tests by developing design recommendations for surface properties.

ACKNOWLEDGMENTS

The author wishes to thank the German Research Foundation (DFG) for funding the research project with the grant code SCHI253/42-1. Further gratitude must be expressed to Dipl.-Ing. Falk Meyer and Dr.-Ing. Andreas Volkwein for their preliminary work in said research project.

ORCID

Kai Osterminski https://orcid.org/0000-0003-0376-0788

REFERENCES

1. DIN 488 1:2009 08. Reinforcing steels–Part 1: Grades, properties, marking. Berlin: Beuth-Verlag, 2009. https://doi.org/10.31030/1520610.
2. DIN EN ISO 15630-1:2019–05. Steel for the reinforcement and prestressing of concrete - Test methods - Part 1: Reinforcing bars, rods and wire (ISO 15630-1:2019); German version EN ISO 15630-1:2019. Berlin: Beuth Verlag; 2019. https://doi.org/10.31030/2885797.
3. Martin, H.; Schießl, P.: Dauerschwingfestigkeit von unbehandelten Betonstählen-Zusammenfassender Überblick über Versuchsergebnisse und theoretische Erkenntnisse-Stand Februar 1975 (German). Institut für Betonstahl und Stahlbetonbau e. V., report No. Sch/K-105/75, 1975.
4. Hanson JM, Burton KT, Hognestad E. Fatigue tests of reinforcing bars–Effect of deformation pattern. J PCA. 1968;10(3):2–13.
5. MacGregor JG, Jhamb IC, Nuttall N. Fatigue strength of hot-rolled reinforcing bars. ACI J. 1971;68(33):169–179.
6. Jhamb, I.C.: Fatigue of reinforcing bars. [Dissertation]. Edmonton, Canada: University of Alberta; 1972.
7. Martin, H.; Schießl, P.: Untersuchungen zur Dauerschwingfestigkeit von dispersionsgehärteten Be-tonrippenstählen BSt 50/55 mit III U- und IV U-Profilierung (German). Institut für Betonstahl und Stahlbetonbau e. V., report No. 18574, 1974.
8. Helgason, T.; Hanson, J.M.; Somes, N.F.; Corley, W.G.; Hognestad, E.: Fatigue strength of high-yield reinforcing bars. Final report No. 164 part 1, National Cooperative Highway Research (NCHR) –Projects 4–7 and 4–7/1 1976.
9. Rehm, G.; Harre, W.; Beul, W.: Schwingfestigkeitsverhalten von Betonstählen unter wirklichkeitsnahen Beanspruchungs- und Umgebungsbedingungen (German). Deutscher Ausschuss für Stahlbeton e.V., No. 374, Beuth, Berlin, 1986. https://doi.org/10.2366/3702642
10. Zheng H, Abel A. Stress concentration and fatigue of profiled reinforcing steels. Int J Fatigue. 1998;20(10):767–773. https://doi.org/10.1016/S0142-1123(98)00051-6.
11. Zheng H, Abel A. Fatigue properties of reinforcing steel produced by TEMPCORE process. J Mater Civ Eng. 1999;11(2):158–165. https://doi.org/10.1061/(ASCE)0899-1,561(1999)11:2(158).
12. Schießl, P.: Theoretische Überlegungen zum Einfluss der Rippengeometrie auf die Dauerschwingfestigkeit von Betonstählen (German). Institut für Betonstahl und Stahlbetonbau e. V., report No. Sch/Me-32/74, 1974.
13. Osterminski K, Gehlen C. Development of a laser-based line scan (LLS) measurement system for surface characterization of reinforcing steel. Mater Test. 2019;61(11):1051–1055. https://doi.org/10.3139/120.111418.
14. DIN 488–2:2009–08. Betonstahl – Betonstabstahl (German). Berlin: Beuth Verlag; 2009. https://doi.org/10.31030/1520611.

AUTHOR BIOGRAPHY

Kai Osterminski
Head of Steel and Corrosion
Chair of Materials Science and Testing
Technical University of Munich
Munich, Germany
kai.osterminski@tum.de

How to cite this article: Osterminski K. Probabilistic modeling of reinforcing bar fatigue on the basis of surface topography data. *Structural Concrete*. 2020;1–8. https://doi.org/10.1002/suco.202000121